

Laboratory Investigations of the Hydrodynamics and Radar Backscattering Properties of Breaking Waves

Guy Meadows¹, Eric B. Dano¹, David R. Lyzenga¹, Hans VanSumeren¹,
Robert Onstott² and Donald E. Lund¹

¹The University of Michigan
Department of Naval Architecture and Marine Engineering
Ann Arbor, MI 48109-2145
PH: (313) 764-6470, FAX: (313) 936-8820;
EMAIL: gmeadows@engin.umich.edu,cbd@engin.umich.edu,lyzenga@umich.edu,vansumer@engin.umich.edu,
dlund@engin.umich.edu

²The Environmental Research Institute of Michigan, Center For Earth Sciences
P.O. Box 134001 Ann Arbor, MI 48113-4001
PH: (313) 994-1200 x2544, FAX: (313) 665-6559; EMAIL: onstott@erim.org

Laboratory Investigations of the Hydrodynamics and Radar Backscattering Properties of Breaking Waves

Guy Meadows¹, Eric B. Dano¹, David R. Lyzenga¹, Hans VanSumeren¹,
Robert Onstott² and Donald E. Lund¹

¹The University of Michigan
Department of Naval Architecture and Marine Engineering
Ann Arbor, MI. 48109-2145
PH: (313) 764-6470, FAX: (313) 936-8820;
EMAIL : gmeadows@engin.umich.edu, ebd@engin.umich.edu, lyzenga@umich.edu, vansumer@engin.umich.edu,
dlund@engin.umich.edu

²The Environmental Research Institute of Michigan, Center For Earth Sciences
P.O. Box 134001 Ann Arbor, MI. 48113-4001
PH: (313) 994-1200 x2544, FAX: (313) 665-6559; EMAIL : onstott@erim.org

Abstract – An experiment was conducted in a 110m x 7.6m x 4m deep Marine Hydrodynamics facility to study the hydrodynamics of intermediate scale breaking waves and how they effect radar backscatter. An energetic spilling breaking wave, characterized by considerable whitecapping, was chosen for analysis. To characterize the wave, an array of seven capacitance wave probes were placed throughout the test basin. The waveprobes observed the temporal evolution of the breaking waves at multiple spatial locations, and were used to determine the spectral content of the pre and post-breaking small scale roughness. Wave probe data showed that the breaking wave reached its greatest amplitude at breaking and then decreased rapidly thereafter. Spectral analysis of the waveprobe data showed that prior to wave breaking, the spectral wave energy was confined to the low frequency wave components of the generated wave group. After breaking, some energy was transferred to high frequency waves, and some energy was dissipated. The energy transferred to the high frequency waves appeared as small scale roughness and was found to influence the radar backscatter.

EXPERIMENTAL DESIGN

Capacitance waveprobes were used as the primary wave characterization sensors in this experiment. Wave probes determine the instantaneous wave height at a point by comparing the outputs of an internally mounted local oscillator and variable oscillator. The variable oscillator is connected to a wave probe element (acting as a variable capacitor) and changes its output frequency based upon the instantaneous water height on the probe. The outputs of the two oscillators are then mixed and converted to a voltage, linearly proportional to the wave height. The wave probes were sampled at 100 Hz., and were accurate to 0.5 mm.

Waveprobe locations were referenced to the wavemaker, and are listed in Table 1.

The breaking waves were generated using a wedge shaped wave maker with a 30 degree face. The wavemaker was programmed to produce a sinusoidal output that was linearly decreasing over a small bandpass of frequencies. The frequency components were chosen, based upon linear wave theory, to create waves that would add constructively and break at a given location [1]. The spilling breaking waves were generated using frequencies from 0.75 Hz to 1.2 Hz. Waves produced at these frequencies ranged from deep to intermediate depth gravity waves. Using linear wave theory and the deep water approximation, the maximum phase speed can be found to equal 2.08 m/s. [2].

To ensure the repeatability of each run, both intrusive (capacitance wave probes) and nonintrusive (laser sheet and video) techniques were used to monitor the waves. The water level was maintained at a constant level throughout the experiment and cleaned with several surface skimmers between each series of runs.

A comprehensive description of the radar and how it was positioned in this experiment is found in [3].

Table 1.

	Downrange Distance
Wavemaker	0 m
Waveprobe #1	7.6 m
Waveprobe #2	11.4 m
Point of Breaking	20.7m
Waveprobes #3,4	20.9 m
Waveprobes #5,6	21.0 m
Waveprobes #7	23.8 m

TEMPORAL DATA

The time series data from the waves probes was used for several purposes. Time plots of waveprobes nearest the wavemaker (#s 1 and 2), were used to monitor the consistency of the generated wave group and ensure the repeatability of all runs. The wave probes nearest wave breaking (#s 3, 4, 5 and 6), were used to analyze the shape of the wave at breaking. Fig. 1 shows a representative waveprobe measurement 20 cm past breaking (as defined by initial roughness on the wave face). This measurement was taken prior to the collapse of the wave crest. As can be seen, the breaking wave is highly peaked and has achieved the highest amplitude in the wave group ($t=33.6$ sec). Video analysis of the breaking wave found the wave crest collapsed 30 cm beyond breaking. At this point, the wave amplitude decayed rapidly to approximately one fifth of its peak amplitude. The wave then continued to propagate down the tow tank with a constant amplitude rounded crest (Fig. 2, $t=35$ sec).

SPECTRAL DATA

The temporal data from all the waveprobes were Fast Fourier Transformed (FFT) over 0.64 second intervals, and then averaged over 64 FFTs. This technique greatly reduced the speckle in the data and yielded resolutions of 1.56 Hz. Representative plots of the waveprobes power spectral densities are shown for a pre-breaking case, and two post-breaking cases with increasing distances from the point of breaking (Fig. 2).

The power in the pre-breaking spectrum is primarily confined to a frequency range of 0.75 to 1.2 Hz. This is the range of wave frequencies generated by the wavemaker, and could be expected. The power drops off rapidly beyond these frequencies and may be considered the high frequency noise floor for the waveprobe measurements. Integrating over the whole pre-break spectrum yields a total spectral power of 44.31 cm^2 (6.87 in^2). This power was constant in the waveprobes located prior to breaking (#s 1 and 2) and will act as a reference for total wave group power.

To analyze the evolution of the breaking waves, a two-scale approach will be utilized. Waves of frequency less than 2 Hz will be considered "low" frequency, whereas waves with frequencies greater than 2 Hz will be considered "high" frequency. This analysis yields a low frequency wave power of 44.25 cm^2 (6.86 in^2), and a high frequency wave power of 0.06 cm^2 ($.01 \text{ in}^2$) for the pre-breaking case.

The first post-break spectrum was from a waveprobe located 30 cm past wave breaking. As discussed previously, the wave crest was collapsing and the amount of small scale roughness was observed to increase dramatically at this point. The spectral power attributed to the post-break

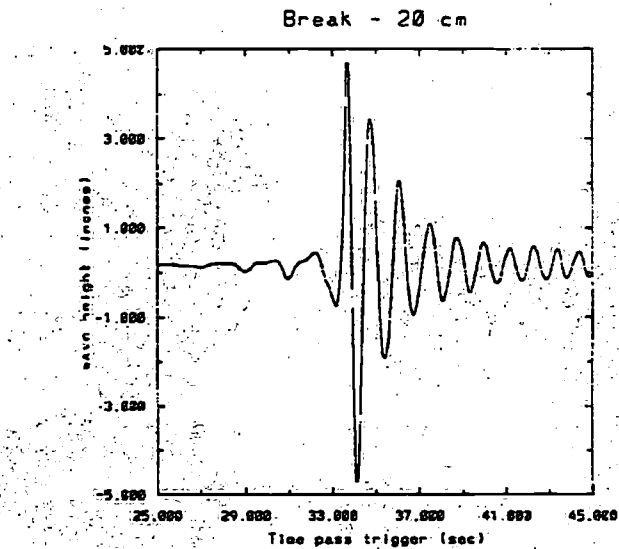


Fig. 1

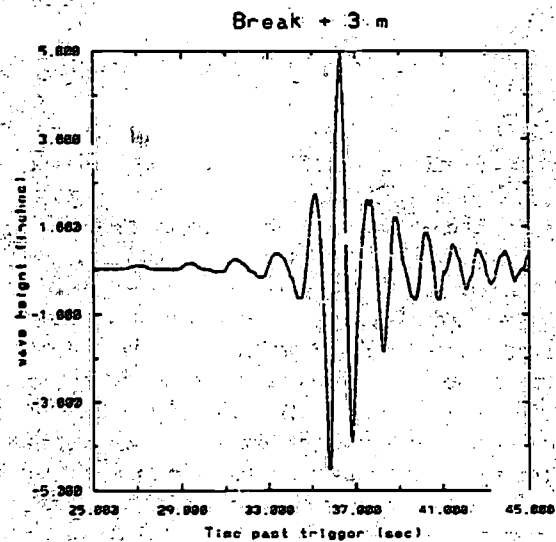


Fig. 2

roughness, is distributed from 4 to 15 Hz.

Integrating the spectral density over frequency yields a total spectral power of 33.23 cm^2 (5.15 in^2). This is a 25% reduction in total wave group power, and indicates that power is dissipated away very early in the wave breaking process. This case yields a low frequency wave power of 32.97 cm^2 (5.11 in^2), and a high frequency wave power of 0.26 cm^2 (0.04 in^2). This indicates that some power has been transferred from the low to high frequency waves.

The second post-break spectrum was from a waveprobe located 3 m from breaking. The total spectral power for this

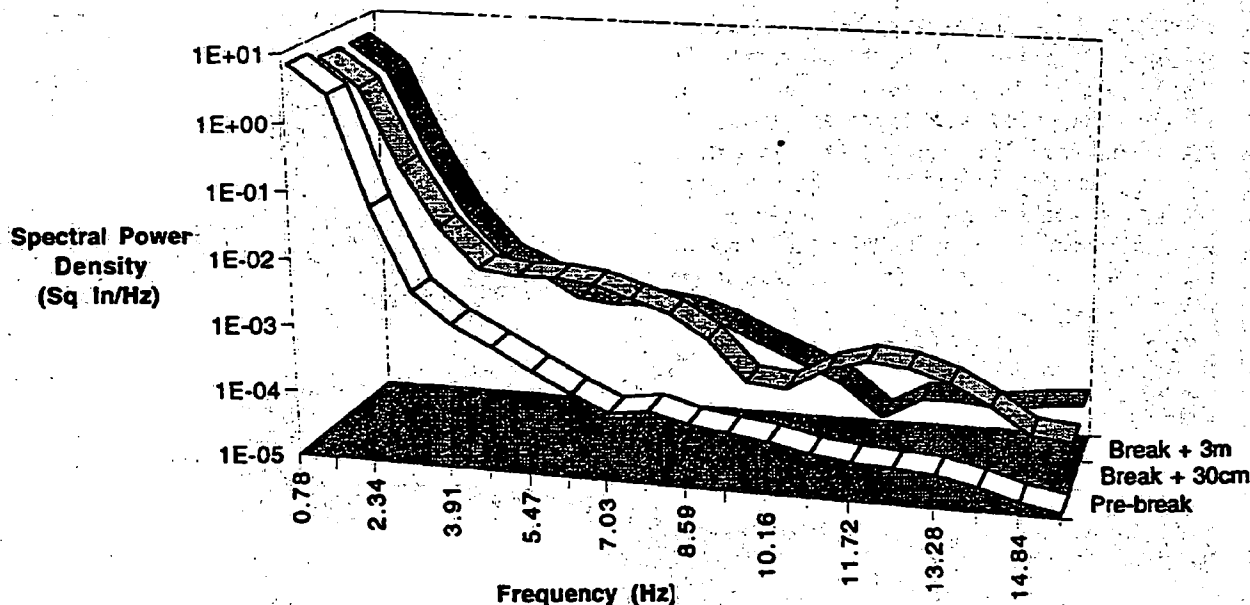


Fig. 3 Power Spectral Densities of the Spilling Breaking Wave.

case was found to be 32.77 cm² (5.08 in²). This shows that an additional 1.0% of the initial wave group power dissipates between 30 cm and 3 m after breaking. The power in the low frequency waves was found to have increased 10% from the last waveprobe. This can be attributed to the growth of other waves in the wave group, and is evidenced in Fig. 2 ($t=36.2$ sec). The high frequency waves decreased in power from the last wave probe to a value of 0.13 cm² (0.02 in²). This is due to the rapid decay of the high frequency waves generated by wave breaking.

The post-break roughness was shown to influence the radar backscatter at several azimuth angles [3], and may be correlated to high frequency wave spectral power.

CONCLUSIONS

Temporal and spectral data were presented from several wave probes used to characterize an energetic spilling breaking wave. The breaking wave was shown to have its maximum amplitude at breaking and to quickly collapse 30 cm past breaking. The total power of the wave decreased throughout breaking, dissipating 25% of the original wave group power within the first 30 cm of breaking, and an additional 1.0% in the next 3 m.

A two-scale approach was taken to analyze the waveprobe spectra, with 2 Hz separating the low and high frequency wave regions. The low frequency waves decreased in power after breaking, but then increased as other waves in the

wave group steepened. The high frequency waves increased in power after breaking, but then decreased as the small amplitude waves decayed.

The amount of power in the high frequency waves appears to correlate with backscattered power from the post-break small scale roughness, and will be a subject of future research.

ACKNOWLEDGMENTS

This research was funded under the Office of Naval Research, Contract # N00014-92-5-1650. The authors would also like to thank Messon Gbah and Lorelle Meadows for their help in processing the wave probe data.

REFERENCES

- [1] M. Davis and E. Zarnick, "Testing ship models in transient waves," Proceedings 5th Symp. Naval Hydro., p507, 1964.
- [2] G. Crapper, "Introduction to Water Waves," John Wiley & Sons, New York, p. 35, 1984.
- [3] E. Dano, D. Lyzenga and G. Meadows, "Doppler characteristics and angular dependence of radar backscatter from laboratory breaking waves," Proceedings 1996 IEEE IGARSS, in press.